*Ecological Applications*, 12(5), 2002, pp. 1496–1509


# CONTRASTING IMPACTS OF A NATIVE AND ALIEN MACROPHYTE ON DISSOLVED OXYGEN IN A LARGE RIVER

NINA F. CARACO[1] AND JONATHAN J. COLE

*Institute of Ecosystem Studies, Box AB, Millbrook, New York 12545 USA*

*Abstract.* In aquatic systems low dissolved oxygen (DO) has been identified as a serious water quality problem. Here we use empirical data and modeling to explore the hypothesis that the introduction of an alien aquatic macrophyte (*Trapa natans*) may have had dramatic impacts on the frequency and extent of low DO events in the Hudson River. Continuous measurements with moored instruments demonstrated that in large macrophyte beds dominated by a native species (*Vallisneria americana*) DO never declined below 5 mg/L during the summer growing season. In contrast, during this same time period, extremely low DO was common in large beds dominated by *Trapa natans*, with DO values below 2.5 mg/L occurring up to 40% of the time. This difference in DO can be modeled based on species differences in the balance of respiration and in-water photosynthesis. The low DO values in *Trapa* beds suggest that these beds may be poor habitats for sensitive fish and invertebrates and that redox sensitive chemical reactions may be altered within *Trapa* beds.

*Key words:* *aquatic plants; Hudson River; hypoxia; introduced species; oxygen dynamics;* Trapa natans; Vallisneria americana.

## INTRODUCTION

The vegetated areas in aquatic systems can be important to ecosystem function in lakes, rivers, and estuaries (Wetzel 1983, Kemp et al. 1984). Macrophyte beds generally have high primary production (Sondergaard and Sand-Jensen 1979, Wetzel 1983) and can, thus, be important sources of organic matter, supporting higher trophic levels and influencing the net metabolism of aquatic systems (France 1995, Duarte and Cebrian 1996). Further, beds can trap sediment, be sites of intense nutrient cycling, and provide important habitat for fish and invertebrates (Carpenter 1980, Graneli and Solander 1988, Garritt 1990, Kiviat 1993, Welcomme 1995, Wilcock et al. 1999).

An important characteristic of macrophyte beds that can alter nutrient cycling and the quality of beds as habitats for fish and invertebrates is dissolved oxygen (DO). When DO falls below 5 mg/L (156 μmol/L), sensitive species of fish and invertebrates can be negatively impacted. At DO levels below 2.5 mg/L most fish are negatively impacted (Frodge et al. 1990). DO can also impact biogeochemical reactions. Prolonged low DO events may lower nitrification and denitrification (Kemp et al. 1990), while short time scale alternation between oxic and hypoxic conditions can enhance denitrification (Knowles 1982). Further, low DO may increase metal and P release from sediments (Lovley 1993). Low levels of DO can occur regularly in bottom waters of aquatic systems (Wetzel 1983, Rabalais et al. 1996) or throughout the water column in systems with heavy organic loads (Clark et al. 1995). They can also be associated with macrophyte beds (Suthers and Gee 1986, Moore et al. 1994, Miranda and Hodges 2000, Miranda et al. 2000).

Low DO events have been reported for thick beds of submerged aquatic vegetation at dawn or during fall senescence (Kaenel et al. 2000, Miranda and Hodges 2000). Emergent and floating-leaved vegetation may, however, be more likely to be associated with persistent or frequent low DO (Frodge et al. 1990). Some floating-leaved macrophytes vent much of their photosynthetically produced oxygen directly into the atmosphere rather than into the water column (Pokorny and Rejmankova 1984). Further, the densely packed canopy of floating leaves severely lowers light beneath it, shading out photosynthesis by any submergent leaves or attached algae (Cataneo et al. 1998). Lastly, the dense canopies of floating-leaved macrophytes can prohibit gas exchange and make more severe low DO generated by negative net ecosystem production in the water column.

The proportion of emergent- to floating-leaved macrophytes in a system can change over time, and this change can be human induced. Humans can alter the hydrologic or nutrient regime, and these changes can be more favorable to one growth form than another (Valiela et al. 1992, Kiviat 1993). Humans can also directly impact the abundance of macrophyte growth forms via species introductions (Kiviat 1993). In the Hudson the introduction of the Eurasian Water Chestnut (*Trapa natans*), which has both floating and submersed leaves, appears to have occurred at the expense of native macrophytes, which were completely submersed (Kiviat 1993).

The tidal portion of the Hudson River has approximately a 1-m tidal range over its 240-km length, which

Manuscript received 6 May 2001; revised 25 October 2001; accepted 30 October 2001; final version received 14 December 2001.

[1] E-mail: caracon@ecostudies.org

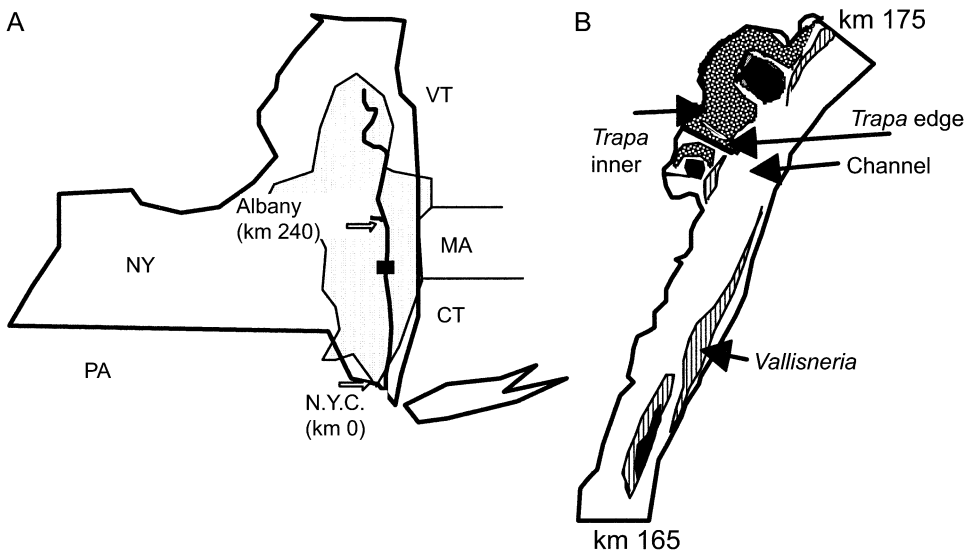


FIG. 1. (A) Location of the tidal Hudson River, which runs south from Albany to New York City, New York (river km 0). The box represents the location of the intensive study site depicted in panel B. (B) Ten-kilometer stretch of the tidal Hudson River where intensive DO study took place during summer 2000. Hatched areas are *Vallisneria* beds, dark stippled areas *Trapa* beds, black is intertidal or permanently exposed islands or jetties, and white represents open water sites. The four sites where sondes were deployed are indicated by arrows.

extends from Albany to New York City (Limburg et al. 1986; Fig. 1). The northern 140-km stretch is fresh water. For this stretch, 70% of the freshwater flow originates from inputs from the Mohawk and upper (nontidal) Hudson River (Lampman et al. 1999). *Trapa* was introduced to the Hudson's watershed as early as 1879; a 1934 survey showed *Trapa* to be abundant in the Mohawk River but did not detect *Trapa* in the tidal Hudson itself (Muenscher 1935, 1937). At this time species found to be abundant in the subtidal regions of the tidal Hudson had submersed leaves only and included *Vallisneria americana*, *Potomogeton perfoliatus* L. var. *bupleruoides*, *Ceratophyllum demsersum*, *Najas* sp., and *Elodea occidentalis* (Muenscher 1935, 1937). At present, *Trapa* is the second most abundant macrophyte in the tidal freshwater Hudson (Findlay, S., E. Blair, W. C. Nieder, E. Branaba, and S. Hoskins, 1997 *unpublished report* to New York Sea Grant, Stony Brook University, Stony Brook, New York).

Macrophytes in the tidal freshwater Hudson occupy ~16% of the surface area of the river and are dominated by two species that occur in distinct, nearly monospecific beds. *Vallisneria americana* covers ~10% of the surface area of the tidal Hudson and is most abundant in water between 0.5 and 1 m depth (Harley and Findlay 1994). *Vallisneria* is a native plant with submersed ribbon-like leaves. Plants are perennial and new leaves arise from overwintering roots in May to June. From late-July to mid-September biomass is maintained at peak dry mass abundance of up to 400 g/m (Harley and Findlay 1994). Beds of *Trapa natans* cover ~6% of the surface area of the tidal Hudson and, like *Vallisneria*, this plant is most abundant in shallow subtidal areas. *Trapa* has both floating rosette leaves that are held up by inflated leafstalks and submersed feather leaves. Plants are annual and sprout from large four-spined seeds in May and by mid June rosette leaves have broken to the surface of all but the deepest sites where growth occurs. From late July to mid-September, biomass is maintained at near peak dry biomass of up to 2000 g/m$^2$ (Kiviat 1993).

In this study we examine the differences in DO dynamics in *Trapa* and *Vallisneria* beds with open exchange to the main channel of the Hudson. The study focuses on sites that were located in close proximity to each other (Fig. 1), and high frequency DO measurements were made simultaneously at these sites using moored, automatically recording instruments. Because between-site differences in DO could be driven by a number of factors, we investigate the potential direct contribution of different plant species by use of modeling based on physiological measurements. We then compare the DO dynamics predicted by our model with those measured in the beds.

## METHODS

### *Metabolism measurements*

Within macrophyte beds we estimated sediment, water column, and macrophyte metabolism (Fig. 2). Macrophyte production and respiration were based on estimates of the biomass of photosynthetic and nonphotosynthetic plant tissue and laboratory measurements of biomass-specific metabolism of these tissues. For *Vallisneria*, plant tissue included roots and leaves. *Trapa* plant tissues include roots, stem, air bladders, rosette

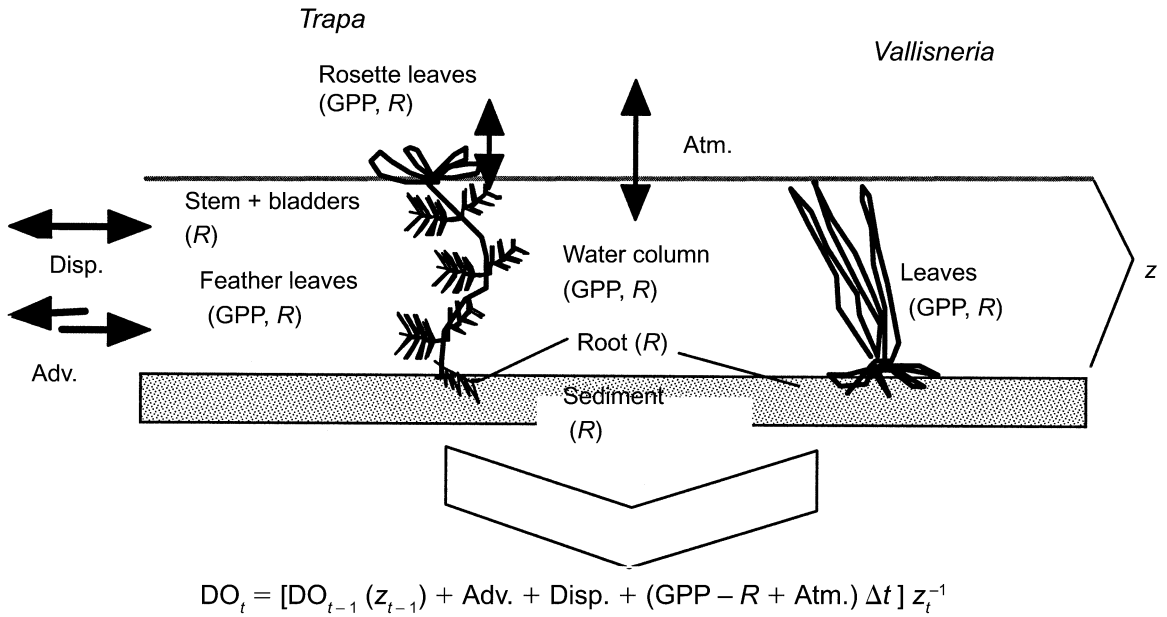


FIG. 2. Components of dissolved oxygen (DO) model for *Trapa* (left) and *Vallisneria* (right) plants. The model includes gross primary production (GPP) and respiration (*R*) of plants tissues, sediment, and water. Total GPP minus *R* is net ecosystem production (NEP). The model also considers water exchange by advection (Adv.), dispersion (Disp.), and atmospheric exchange (Atm.). The model is run on a 0.25-h time step ($\Delta t$) and 0.1-m depth ($z$) step.

leaves, and feather leaves (Fig. 2). In the case of air bladders we assumed respiration equal to that measured in stems, as the high air storage in these tissues made short-term metabolic estimates unfeasible.

Estimates of macrophyte tissue respiration and production were based on DO changes in incubations in the dark and over a light gradient, respectively (Harley and Findlay 1994). For these incubations we collected intact macrophytes during early morning. Material was transferred to coolers filled with Hudson River water and transported to the laboratory where plants were cut into separate tissue parts (Table 1). Separate Hudson River water was collected the prior evening and filtered with Whatman GF/F glass fiber filters (Whatman Scientific, Kent, UK). Immediately before incubations, this water was siphoned into 300-mL BOD bottles while being mixed to assure even distribution of initial DO between bottles. The remaining bottles were water controls or included plant tissue (dry mass ~50 mg).

Incubations were 3 h, during which temperatures were within 1°C of ambient river temperatures (~22°C). DO consumption in dark bottles was estimated for photosynthetic and nonphotosynthetic tissue (Table 1). For the photosynthetic tissues (leaves) we also determined net DO production at eight levels of photosynthetically active photons, varying between 15 and 2000 $\mu mol \cdot m^{-2} \cdot s^{-1}$. Light levels were created with neutral-density screening as has been done to measure phytoplankton photosynthetic parameters in the Hudson (Cole et al. 1992). At the end of all incubations, plant material was carefully removed and dried in order to transform DO changes to mass-specific rates. After plant material had been removed, DO was fixed immediately by the addition of manganese and base Winkler reagents and within 24 h DO was measured following sample acidification (Roland et al. 1999).

For *Trapa*, biomass of photosynthetic and nonphotosynthetic tissue in beds was based on estimates of

TABLE 1. Measured tissue respiration and areal biomass of *Trapa* and *Vallisneria* tissue. These two measurements are used to calculate the areal respiration of each plant tissue.

| Plant | Tissue | Dry-mass tissue respiration (mg $O_2 \cdot g^{-1} \cdot h^{-1}$) | Dry biomass ($mg/m^2$) | Respiration (g $O_2 \cdot m^{-2} \cdot h^{-1}$) |
|---|---|---|---|---|
| *Trapa* | rosette leaves† | 0.6 | 355 | 0.21 |
| | feather leaves | 1.6 | 95 | 0.15 |
| | stems + bladders | 0.7 | 190 | 0.13 |
| | roots | 0.6 | 10 | 0.01 |
| *Vallisneria* | leaves | 1.0 | 70 | 0.07 |
| | roots | 0.7 | 30 | 0.02 |

† These floating leaves may not contribute to the water column DO dynamics.

rosette leaf density in beds and biomass of plant parts associated with each rosette leaf. On 11 August floating rosette leaf density was obtained at five locations within the bed by counting abundance of rosettes within a 0.5-$m^2$ frame. The biomass of plant tissue parts per rosette was based on whole plants harvested for photosynthetic experiments. Five plants were divided into component parts and dry mass of each part was obtained. For *Vallisneria*, biomass of roots and stems was calculated as the average total biomass in beds between 0.5 and 1.5 m depth (Harley and Findlay 1994) and estimate of the relative masses of leaf and root from five plants harvested for photosynthetic measurements. These plants were also used to get average height of plants in the beds.

To estimate sediment respiration, we relied on previous measurements based on core incubations of subtidal sediment (J. L. Zelenke 1997, *unpublished report* to the Hudson River Foundation [40 West 20th Street, New York, New York]: Tidal freshwater marshes of the Hudson River as nutrient sinks: long-term retention and denitrification). These measurements suggest a sediment respiration of on average 0.8 g $O_2 \cdot m^{-2} \cdot d^{-1}$. We assumed that photosynthesis on sediments was negligible in both beds. Water column respiration at both sites was assumed to be equal to volumetric respiration in open water sites of the Hudson, or $\sim$0.3 g $O_2 \cdot m^{-3} \cdot d^{-1}$ (Caraco et al. 2000). Water column photosynthesis was based on photosynthetic parameters of phytoplankton in the Hudson (Cole et al. 1992, Caraco et al. 1997) and models of light in the macrophyte beds (below).

### *Field measurements*

DO was measured at five sites with automatically recording YSI Endico sondes (UPG 6000 with pulsed $O_2$ electrodes; Yellow Springs Instrument, Yellow Springs, Ohio, USA). In addition to DO, sondes recorded temperature and water depth. Further, in some deployments sondes were equipped with turbidity sensors. Turbidity was standardized to a 20 NTU standard prior to each 5- to 15-d deployment. DO was standardized to atmospheric saturation at the beginning of deployments. Electrode drift during deployment was detected by air saturation measurements at the end of deployment (Cole et al. 2000). Drift averaged 4% during deployments and never exceeded 13%. Errors associated with drift were corrected for by a linear interpretation routine.

During 1999, a single sonde was deployed in a 0.9-$km^2$ *Trapa* bed located at km 139 of the Hudson River for 4 d in late July. Measurements were made at 5-min intervals during this deployment. During summer 2000, extensive measurements were made at a larger (1.1-$km^2$) *Trapa* bed centered at km 173 with simultaneous measurements being made in a 0.6 $km^2$ *Vallisneria* bed, and an adjacent open-water site in the tidal Hudson River (Fig. 1). For the *Trapa* site, we monitored DO at two locations: one located at the edge of the *Trapa* bed (close to open water, Fig. 1) and one at a more interior site in the bed. This site was accessed through a narrow channel that runs into the bed. In all macrophyte sites during 2000, measurements were made at 10-min intervals for 32 d in July to August (three 10- to 12-d deployments) and 34 d (three 10- to 12-d deployments) in September to October at both the *Trapa* and *Vallisneria* sites. For the open water site, measurements were continuous for July through early October and were made at 15-min intervals with deployments averaging 2 wk. Water depth at the open water site was 9 m at mean low tide, and sondes were deployed at 2 m. Average depth in macrophyte beds ranged from 0.2 to 0.8 m at mean low tide. Sondes were deployed from 0.15 to 0.5 m above the sediment at these sites. When sondes were deployed DO was also measured with newly programmed sondes reading at 1-min intervals or with portable YSI meters. These measurements were within 0.3 mg/L of DO measured on moored sondes at the same time.

In addition to intensive measurements made with deployed sondes, transects were run from adjoining open waters into *Trapa* and *Vallisneria* beds during August 1999 and 2000. Sondes programmed to take measurements at 1-min intervals were slowly towed from open waters into macrophyte beds. All measurements were at $\sim$0.2 m depth. The transect sites included the three large beds where we had moored sondes, six additional *Trapa* sites that ranged in size from $<$0.1 to 0.4 $km^2$, and four additional *Vallisneria* sites that ranged in size from 0.3 to 0.7 $km^2$.

Light measurements were made using a LI-COR model LI-193SB spherical quantum sensor (LI-COR, Lincoln, Nebraska, USA) with a model LI-1000 data logger (Cole et al. 1992) within our intensively studied macrophyte beds and the adjoining channel (Fig. 1). Measurements were made on 11 August when macrophyte biomass had reached peak values. Measurements were made in air and at 0.1-m depth intervals to the base of the water column. Lastly, on three dates from July to September 2000, samples were taken during ebbing tide in the mid-*Trapa* site and adjacent channel site (Fig. 1) for analysis of nitrate, ammonium, total N, phosphate, and total P (Lampman et al. 1999).

### *Modeling DO dynamics*

We modeled DO dynamics in both *Trapa* and *Vallisneria* beds. In the model, changes in DO are a function of respiration ($R$) and gross primary production (GPP), horizontal advection (Adv.) and dispersion (Disp.), and air–water exchange (Atm.) as they change with both diurnal and tidal variation in light and depth (Fig. 2). Depth ($z$) variation influenced not only the light regime of plants and the extent to which areal based metabolism was concentrated in the water column but in addition determined advective inputs of water and DO from the adjoining channel. The model was run at a 15-min time step ($\Delta t$). Light and GPP were

calculated at 0.1-m depth intervals from 0 m to the maximum depth of the water column and were summed for each time step. Adv. and Disp. are in grams per square meter input per time step. GPP, *R*, and Atm. are in grams per square meter per hour. DO is in milligrams per liter (grams per cubic meter). The model was initialized with a DO of 7.5 mg/L (channel DO concentrations during model run) and run for 2 d to allow model equilibrium before modeling days to be compared to output data. As our physiological and light data within macrophyte beds was taken during July–early August, we show model results only for this time period.

The 1-m tidal range in depth of the water column was modeled as a sine function of time of day and day such that

$$\text{depth}_t = \text{average depth} + 0.5 \sin[0.5(\text{time} - \text{day of year} - 205)] \quad (1)$$

where average depth is the depth at mid-tide in the macrophyte bed in meters. This function allowed tide to advance 1 h per day but did not take into account daily asynchronies that can occur in the river. The input of channel water to the beds during flooding tide (Adv.(In)) was calculated as:

$$\text{Adv.(In)} = \text{DO}_{\text{channel}}(z_t - z_{t-1}) \quad (2)$$

where $\text{DO}_{\text{channel}}$ is the DO concentration in the channel (7.5 mg/L in these model runs) and $z_t$ and $z_{t-1}$ are the modeled depths of the water between time steps. Similarly the output of DO with ebbing tide is

$$\text{Adv.(Out)} = \text{DO}_{t-1}(z_{t-1} - z_t) \quad (3)$$

where $\text{DO}_{t-1}$ is the DO in the macrophyte bed at time $t-1$.

In addition to the above unidirectional inputs of water during flooding and ebbing tides, water may exchange with the channel by dispersion (Disp.). We assumed that this exchange was proportional to velocity and a function of tidal exchange. Such that

$$\text{Disp.} = \text{ABSOLUTE}(z_t - z_{t-1})F(\text{DO}_{\text{channel}} - \text{DO}_{t-1}) \quad (4)$$

where *F* is a dimensionless constant that we varied in different model runs from zero (no dispersive exchange) to three (dispersive water exchange threefold advective exchange). Atmospheric inputs to the bed (Atm.) were calculated as

$$\text{Atm.} = k(\text{DO}_{\text{atm}} - \text{DO}_{t-1}) \quad (5)$$

where $\text{DO}_{\text{atm}}$ is the concentration of DO associated with atmospherically equilibrated water and *k* is piston velocity for air–water exchange, which was varied from 0 to 0.033 m/h in different model runs. These values represent minimum and maximum scenarios as the exchange in the quiescent waters of the macrophyte beds was likely less than the ~0.033 m/h exchange found in the Hudson River (Caraco et al. 1999).

The incoming potential radiation was modeled at each time step according to Iqbal (1983) as a function of latitude and day of year. Based on light measurements made at the Institute of Ecosystem Studies (Kelly 1993), actual incident light ($I_s$), was estimated as 60% of potential. Light with depth ($I_z$) was modeled from time dependent incoming irradiance ($I_s$) and extinction of light such that

$$I_z = I_s T e^{-kdz}. \quad (6)$$

*T* is the fraction of incoming light that is transmitted through surface waters (vs. being reflected or absorbed by floating vegetation), $k_d$ is the light extinction in the water due to plants, particles, and DOM, and *z* is the depth in meters. Parameters were fit for each bed based on light measurements with depth (*Field measurements*, above). We used these fitted parameters for all model scenario runs but one where we increased *T* 10-fold over those based on measurements to simulate production in beds with less plant biomass.

Respiration was assumed to be light-independent and to, therefore, occur at a constant rate throughout the day and over depth (Table 1). Gross primary production of phytoplankton and macrophytes was related to light through a hyperbolic tangent model (Goldsborough and Kemp 1988, Cole et al. 1992, Harley and Findlay 1994). Light varied with depth and time and GPP for each depth and time interval was calculated as

$$\text{GPP}_{t,z} = \text{biomass}_{t,z}\text{GPP}_{\max}\tanh(I_z/I_k). \quad (7)$$

The maximum gross photosynthesis ($\text{GPP}_{\max}$) and the light value where this maximum is approached ($I_k$) were fit using a modified Marquardt procedure to laboratory measurements of DO production (*Metabolism measurements*, above; Cole et al. 1992). $\text{Biomass}_{t,z}$ is the biomass of photosynthetic tissue at each depth interval. To estimate this, submersed leaves were assumed to stand upright in the water column unless the height of plants exceeded the height of the water column, at which point submersed tissue was assumed to bend 90° at the surface. Light for submersed tissue at the surface was, therefore, equal to $TI_s$ (Eq. 6). Light for floating vegetation (*Trapa* rosettes leaves) was modeled as $I_s$.

For all submersed plant tissue (all but *Trapa* rosette leaves) DO produced and consumed by photosynthesis and respiration were assumed to directly and instantaneously contribute to DO changes in the water column. For floating rosette leaves, we ran two extreme model scenarios, first where we assumed that the floating leaves did not contribute to water column DO (all DO produced/consumed was vented to the atmosphere) and second that, like submersed tissue, this DO had a direct and instantaneous effect on water column DO.

## Results

### *Metabolism*

Incubations (3 h each) of plant tissue in the dark resulted in declines of DO that ranged from 1.5 to 5

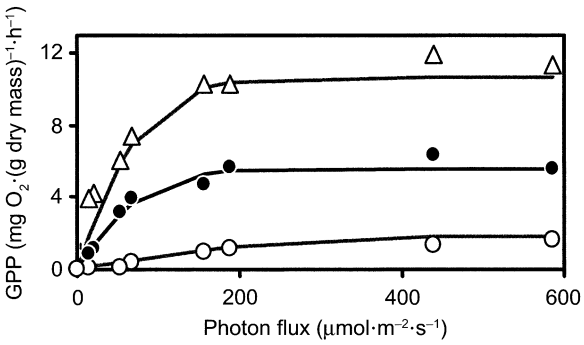


FIG. 3. Gross primary production (GPP) vs. light for *Vallisneria* leaves (triangles), *Trapa* feather leaves (solid circles), and *Trapa* rosette leaves (open circles). Each point is the mean of three replicates, and the CV of points averaged 5% of the mean. Photon flux values extended to 2000 $\mu mol \cdot m^{-2} \cdot s^{-1}$, but we show values only to 600 $\mu mol \cdot m^{-2} \cdot s^{-1}$ so that response at low light can be better seen. The lines are a hyperbolic tangent fit to all data. For *Vallisineria*, *Trapa* feather, and *Trapa* rosette leaves, modeled vs. measured GPP agreed well ($r^2$ = 0.96, 0.97, and 0.96, respectively).

mg/L. Dark incubation of filtered Hudson River water (e.g., controls without plant material) had negligible declines in DO in comparison (<0.1 mg/L). The different plant tissue consumed DO in the dark at rates that varied from 0.5 to 1.6 mg $O_2 \cdot g^{-1} \cdot h^{-1}$. *Trapa* feather leaves had the highest biomass specific respiration (*R*, Table 1).

In the light incubations, for all leaves there was increasing DO production as light increased. The net primary production (NPP) measured by these incubations switched from negative to positive values of photon influx at from 20 to 100 $\mu mol \cdot m^{-2} \cdot s^{-1}$ with higher light values required for this switch in rosette leaves of *Trapa*. At the highest light levels, where DO production was maximum, DO levels rose up to 12 mg/L (140% saturation) during incubations. These values were not so high as to cause DO bubbles to form in the water.

For all three leaves the gross primary production (GPP), calculated as the sum of NPP and *R*, was modeled well by the hyperbolic tangent model (Eq. 7, Fig. 3); <96% of the variation in DO production was explained by this model. The parameters of the model differed somewhat between leaves. $I_k$ of *Trapa* rosette leaves was 250 $\mu mol \cdot m^{-2} \cdot s^{-1}$, while $I_k$ of *Trapa* feather and *Vallisneria* leaves were almost identical at near 85 $\mu mol \cdot m^{-2} \cdot s^{-1}$. $GPP_{max}$ varied substantially among all three leaf types and was 11, 5.5, and 2 mg $O_2 \cdot g^{-1} \cdot h^{-1}$ for the *Vallisneria*, *Trapa* feather, and *Trapa* rosette leaves, respectively. We know of no other studies that have investigated the photosynthetic parameters of *Trapa* leaves. The photosynthetic parameters that we found for *Vallisneria* are very close to those found in a previous study (Harley and Findlay 1994).

High respiration rates in *Trapa* beds were largely due to high plant biomass in these beds, rather than large differences in biomass-specific respiration estimates (Table 1). Estimated biomass of plant tissue was about six-fold greater in the *Trapa* than in the *Vallisneria* bed (Table 1). For *Trapa* <50% of this biomass was in floating leaves, which contribute to the plant's carbon balance but may not contribute to water column DO dynamics. Even considering the submersed biomass, however, *Trapa* biomass was almost three times that of *Vallisneria*. The respiration by plants in *Vallisneria* beds was estimated at 0.1 g $O_2 \cdot m^{-2} \cdot h^{-1}$. The respiration of submersed plant tissue in *Trapa* beds was estimated 0.3 g $O_2 \cdot m^{-2} \cdot h^{-1}$ and the respiration of the total plant was 0.5 g $O_2 \cdot m^{-2} \cdot h^{-1}$. For both macrophyte beds, sediment respiration was estimated at 0.03 g $O_2 \cdot m^{-2} \cdot h^{-1}$ and water column respiration was 0.01 g $O_2 \cdot m^{-2} \cdot h^{-1}$ for a 1-m water column. Considering all components of respiration, *Trapa* beds had two and one-half to five-fold higher respiration than *Vallisneria* beds if we consider submersed vegetation only or include floating leaves in our estimates.

The biomass of submersed photosynthetic tissue (leaves) was ~1.6-fold greater in the *Trapa* as compared to the *Vallisneria* beds, while the production per unit mass of leaf was about twofold greater for *Vallisneria* than for *Trapa* (Fig. 3). Thus, given saturating light levels, GPP of submersed tissue would be 0.7 and 0.6 g $O_2 \cdot m^{-2} \cdot h^{-1}$ for *Vallisneria* and *Trapa*, respectively. If we consider floating leaves in addition, GPP of *Trapa* plants would be 1.3 g $O_2 \cdot m^{-2} \cdot h^{-1}$ at saturating light conditions. By comparison, at the average chlorophyll *a* concentration of 4 mg/$m^3$ (Caraco et al. 1997) and saturating light, we would expect a planktonic DO production of ~0.05 g $O_2 \cdot m^{-2} \cdot h^{-1}$ in a 1-m water column (based on a $GPP_{max}$ of 14 mg $O_2 \cdot$(mg chlorophyll *a*)$^{-1} \cdot h^{-1}$, Cole et al. 1992). The extent to which these maximum productions are approached depends on the light level in macrophyte beds compared to the $I_k$ values for photosynthesis.

### *Light regime*

At a given depth light in the water column of macrophyte beds and in *Trapa* beds in particular is considerably lower than in the main channel of the river. In the open channel, based on light measured with depth (Fig. 4), we estimate *T* and $k_d$ values (Eq. 6) of 0.74 and 2.4 $m^{-1}$ depth, respectively. For *Vallisneria*, we estimate *T* and $k_d$ of 0.55 and 4.1 $m^{-1}$, respectively, while for *Trapa*, these values were 0.01 and 3.9 $m^{-1}$, respectively. Thus, in the channel, *Vallisneria* bed, and *Trapa* bed only 47%, 24%, and 0.5%, respectively, of incident light ($I_s$, Eq. 6) reached 0.2 m depth. For *Trapa* beds, even at 0.05 m (immediately below floating leaves) light would only be 0.8% of $I_s$.

### *DO dynamics*

Continuous DO measurements for 1999 and 2000 show that in the large *Trapa* beds, DO varied dramatically over short time scales and that low DO events were common (Fig. 5). For the 0.9-$km^2$ *Trapa* bed lo-

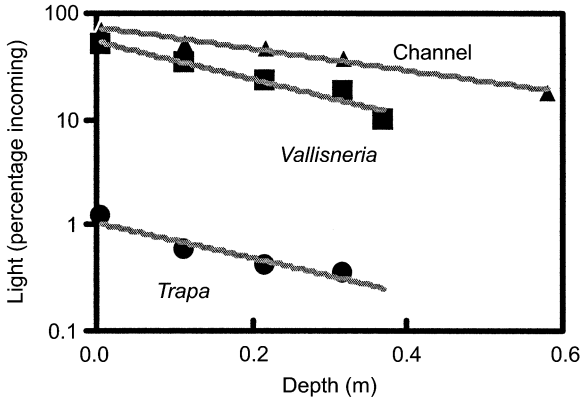


FIG. 4. Measured light over depth in the channel (triangles), *Vallisneria* bed (squares), and *Trapa* bed (circles), expressed as a percentage of incoming photon flux. The lines represent the fit exponential equations. Note the log scale.

cated at km 139, during July 1999 DO varied within a 6-h period between 0 and 8.2 mg/L. For the deployments during July and August 2000 (Fig. 1B), DO varied between 0 and 8.0 mg/L at the edge of the bed and between 0 and 6 mg/L at the inner site. For September to October, DO ranged from 0 to 8.5 mg/L at both the edge and inner sites. Depth profiles suggested that these recorded changes occurred throughout the water column.

In the *Trapa* bed, the variation in DO was not related to a diurnal cycle but occurred on a 12.5-h tidal cycle (Fig. 6A, C). At, or just prior to, high tide DO levels were highest, and at the edge site, were generally coequal with channel values (7–8 mg/L). In the inner site DO values peeked near the same time, but even these peak values were frequently lower than main channel DO values (Fig. 6C). At both inner and edge sites DO declined consistently as tide ebbed, reaching lows of 0 to 2.5 mg/L at low tide. During each flood tide, DO increased rapidly, reaching near peak values ~1 and 3 h after the beginning of flood tide at the edge site and inner sites, respectively (Fig. 6C).

In the *Vallisneria* bed, DO was less dynamic than in the *Trapa* bed. In July–August and September–October, DO varied between 6.3 and 11.8 mg/L and 7.2 and 12.3 mg/L, respectively (Fig. 5, 6B). DO values were generally lowest in late night to early morning and generally increased by 2–4 mg/L to reach peak values during early afternoon to dusk (Fig. 6A, B). The daily cycles were not as regular as the tidal cycles we observed in the *Trapa* bed. This is likely due to the fact

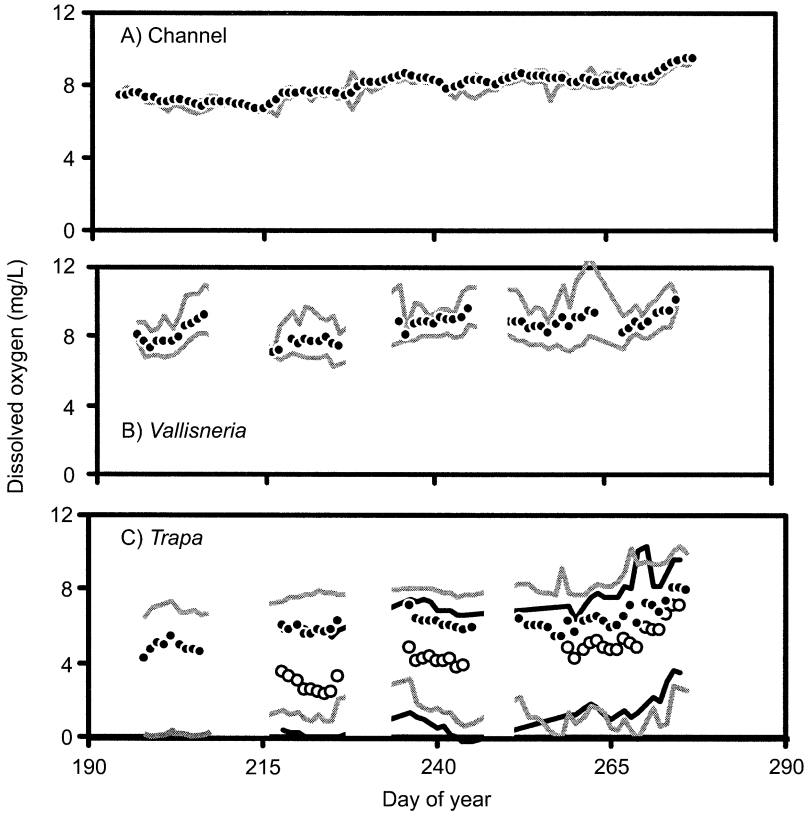


FIG. 5. Average daily DO values (circles) and daily maximum and minimum values (lines) based on measurements made at 10–15 min intervals throughout the day. (A) Channel DO; (B) *Vallisneria* DO; (C) *Trapa* DO. For (C) two sites are represented, a site in the inner part of the *Trapa* bed (black lines and open circles) and a site at the edge of the bed (gray lines and solid circles). These midsummer to fall measurements cover the time of high macrophyte biomass in the river.

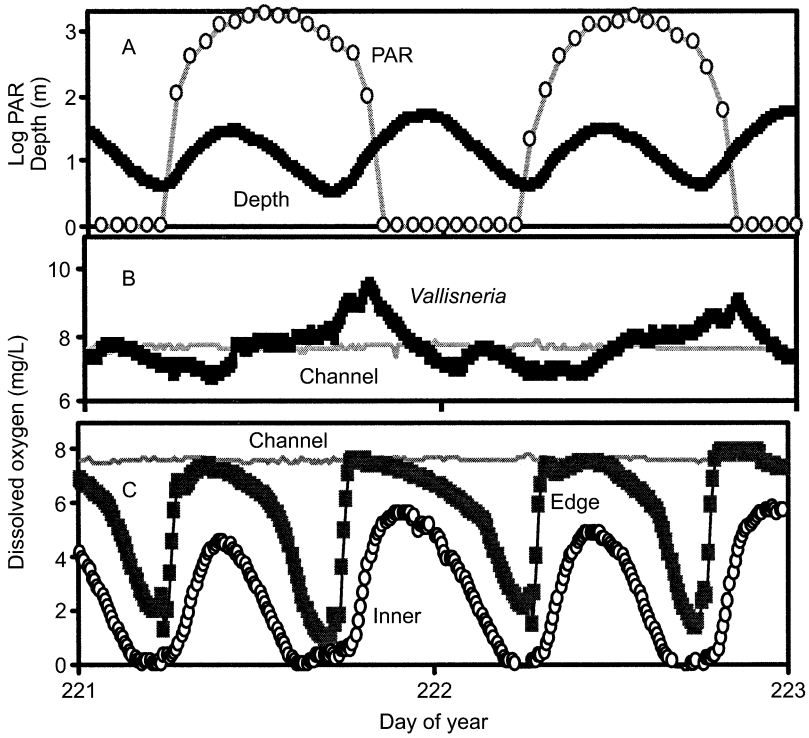


FIG. 6. Measurements of diurnal variation in DO, light, and water column depth for 2 d in midsummer. (A) Variation of incoming photosynthetically active radiation (PAR, circles) and depth of the water column as measured at the edge site in the *Trapa* bed. Note that the PAR values are on a log scale; these values are hourly averages measured at a site 30 km from our study site. (B) DO in *Vallisneria* bed (solid squares) and channel (gray line). (C) DO at the *Trapa* edge site (solid squares), inner site (open circles), and the channel (gray line). Note that the DO in the *Trapa* sites varies with tidal duration, while the DO in the *Vallisneria* site shows a predominantly diurnal pattern.

that *Vallisneria* beds experience tidal flushing asynchronously with diurnal cycles.

In addition to the difference in pattern of DO decline in *Trapa* and *Vallisneria*, the beds have very different frequency of low DO events. In the *Trapa* bed during July 1999, DO values below 5 and 2.5 mg/L occurred 51% and 30% of the time, respectively. Similarly during 2000, for July and August 2000 DO values $<5$ mg/L occurred 31% and 71% of the time for the edge and center sites in the *Trapa* bed, respectively, and values $<2.5$ mg/L occurred 12% and 42% of the time at the edge and center of the *Trapa* beds, respectively. In contrast, for July to August in the *Vallisneria* bed, DO never dropped below 5 mg/L and DO above 7.5 mg/L occurred 65% of the time.

Measurements along transects into macrophyte bed sites show the same species driven difference in DO as we observed from our large intensively studied sites (Fig. 7). That is, compared to open water sites, large *Trapa* beds have substantially lower DO while large *Vallisneria* beds had substantially greater DO than that of adjoining open waters. The DO differences between beds seemed to decline with bed size, and for the small *Trapa* beds we did not find the large DO depletions that were found in the large beds. DO values in these beds were never $<5$ mg/L; the lowest DO value found was 6 mg/L or $\sim$1.5 mg/L lower than the values in the adjoining open water site at this time. These data suggest that the low DO events in *Trapa* beds may be restricted to large beds. These large beds make up $\sim$50% of the total area of *Trapa* in the river.

### *Nutrients*

Nitrogen concentrations in the main channel of the Hudson River were substantially higher than in the *Trapa* bed. During summer 2000 in the channel $NO_3$, $NH_4$, and TN averaged 35, 2.3, and 60 μmol/L, respectively (Fig. 8). These values are close to long-term averages observed in the channel of the Hudson (Lampman et al. 1999). In the *Trapa* bed $NO_3$, $NH_4$, and TN concentrations were 9.0, 1.6, and 30 μmol/L, respectively. Thus, both DIN and TN were depleted during these ebbing tide samples by close to 30 μmol/L with respect to channel concentrations.

Like nitrogen, phosphorus was lower in the *Trapa* bed than in the main channel but depletion was proportionally less. $PO_4$ and TP averaged 0.67 and 1.8 μmol/L in the channel and 0.37 and 0.93 μmol/L in the *Trapa* bed. Thus, the depletions of $PO_4$ and TP were 0.30 and 0.87 μmol/L, respectively. On average, DIN depletion was 90× that of $PO_4$ and TN depletion was 33× that of TP. These depletion values never ap-

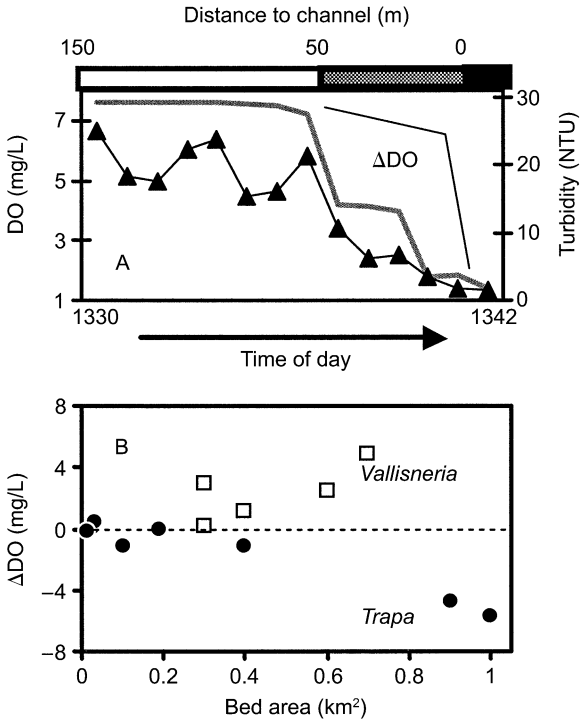


FIG. 7. DO measured along transects in the Hudson. (A) Example of transect of DO (heavy line) and turbidity (triangles) from 3 August 2000. The transect was made by towing a sonde programmed to read at 1-min intervals. The transect runs from the main channel into the vegetated area of a large *Trapa* bed (Fig. 1). At ~50 m a small channel that inundates the *Trapa* bed was reached (gray bar), and the transect ends at the end of this small channel in the thick vegetation of the *Trapa* bed (black bar). ΔDO is considered the difference in DO between the channel and vegetated area of the bed. (B) ΔDO values as measured from sonde transects for eight *Trapa* (circles) and five *Vallisneria* beds (squares) vs. the estimated size of each of the macrophyte beds. The channel DO values during the early August measurements were between 7.1 and 7.6 mg/L.

proached the Redfield ratio of 16 DIN/$PO_4$ and only approached this depletion ratio expected for plant uptake on one date for TN/TP (Fig. 8C). The high depletion of N with respect to P could indicate that part of the uptake within beds is due to denitrification.

### *Model results*

Model scenarios were run for both species, considering different Atm. and Disp. values. In addition, for *Trapa* we ran scenarios with different light input and exclusion or inclusion of emergent tissue in the DO balance. The model was run for 16 d in July (days of year 215–231). For seven of the scenario runs, average predicted daily values of NEP and DO for days 217–231 are presented in Table 2 (*S1–S7*) and detailed results for two days (day of year 221–222) are shown graphically (Fig. 9) and compared to measurements for those same dates (Fig. 6). Although only NEP and DO results are shown in the Table 2 and Fig. 9, we discuss components of the model including GPP, Atm., and Adv.

When the model is run with measured light and photosynthetic parameters (Figs. 3, 4), modeled GPP for *Vallisneria* and *Trapa* averaged 3.6 and 12.6 g $O_2 \cdot m^{-2} \cdot d^{-1}$, respectively. For *Trapa* most of this GPP occurred by floating leaves and GPP of submersed tissue was only 0.5 g $O_2 \cdot m^{-2} \cdot d^{-1}$ or <5% of total GPP. Net ecosystem production (NEP) is GPP minus plant, sediment, and planktonic respiration. Within *Vallisneria* beds hourly NEP varied between −0.2 and 0.5 g $O_2 \cdot m^{-2} \cdot h^{-1}$ throughout the day. Peak values occurred during midday low tides and for day 221, two distinct peaks in NEP occur (Fig. 9A). The average daily NEP for days 217–231 was 0.13 g $O_2 \cdot m^{-2} \cdot d^{-1}$ (Table 2) and the daily NEP varied between −0.06 and 0.29 g $O_2 \cdot m^{-2} \cdot d^{-1}$ depending on the timing of low tides during the day. For *Trapa* beds hourly NEP varied between −0.53 g $O_2 \cdot m^{-2} \cdot h^{-1}$ at night to 0.52 g $O_2 \cdot m^{-2} \cdot h^{-1}$ during daytime (Fig. 9A). Considering only submersed vegetation, hourly NEP was always negative and varied between −0.35 and −0.25 g $O_2 \cdot m^{-2} \cdot h^{-1}$ (9A). The daily average NEP with the inclusion and exclusion of the floating rosette leaves was −0.34 and −7.2 g $O_2 \cdot m^{-2} \cdot d^{-1}$, respectively (Table 2). The metabolic balance for the entire *Trapa* plants (e.g., excluding sediment and planktonic metabolism, Fig. 2) was positive and averaged 0.5 g $O_2 \cdot m^{-2} \cdot d^{-1}$.

Compared to metabolism, atmospheric exchange (Atm.) in the *Vallisneria* bed was relatively low even when *k* values (Eq. 5) used in the model were as high as the more turbulent channel. Atm. varied between 0.04 g $O_2 \cdot m^{-2} \cdot h^{-1}$ near sunrise to −0.05 g $O_2 \cdot m^{-2} \cdot h^{-1}$ prior to sunset. Peak daytime atmospheric exchange is, therefore, ~10% of peak daytime NEP (Fig. 9A). Modeled Atm. in *Trapa* beds was highly dependent on whether floating leaves were considered to contribute to water column DO dynamics. When floating leaves were included in the water column DO model, the model predicts a large diurnal shift in Atm. from −0.3 to 0.3 g $O_2 \cdot m^{-2} \cdot h^{-1}$; when excluded modeled Atm. varied between 0.14 and 0.3 g $O_2 \cdot m^{-2} \cdot h^{-1}$ and variation was related to tidal cycle with highest atmospheric exchange at the end of ebbing tide.

As advective inputs depend only on channel DO values and not DO within the macrophyte beds, Adv. input of DO during flooding tides was the same for all model scenario runs. Adv. reached maximum values during mid flood of 1.8 g $O_2 \cdot m^{-2} \cdot h^{-1}$ and was 7.5 g $O_2 \cdot m^{-2}$ per 6.2-h tidal cycle. These advective inputs would have dramatically different impacts on DO dynamics depending on the ambient DO in the bed. When DO concentrations in the bed were near 7.5 mg/L (channel DO values for the model period), there was little impact; when values of DO in the bed differ greatly from 7.5 mg/L the impact of advective inputs can be substantial. For example, if DO values were 0 mg/L at the beginning of low tide and depth of the water column

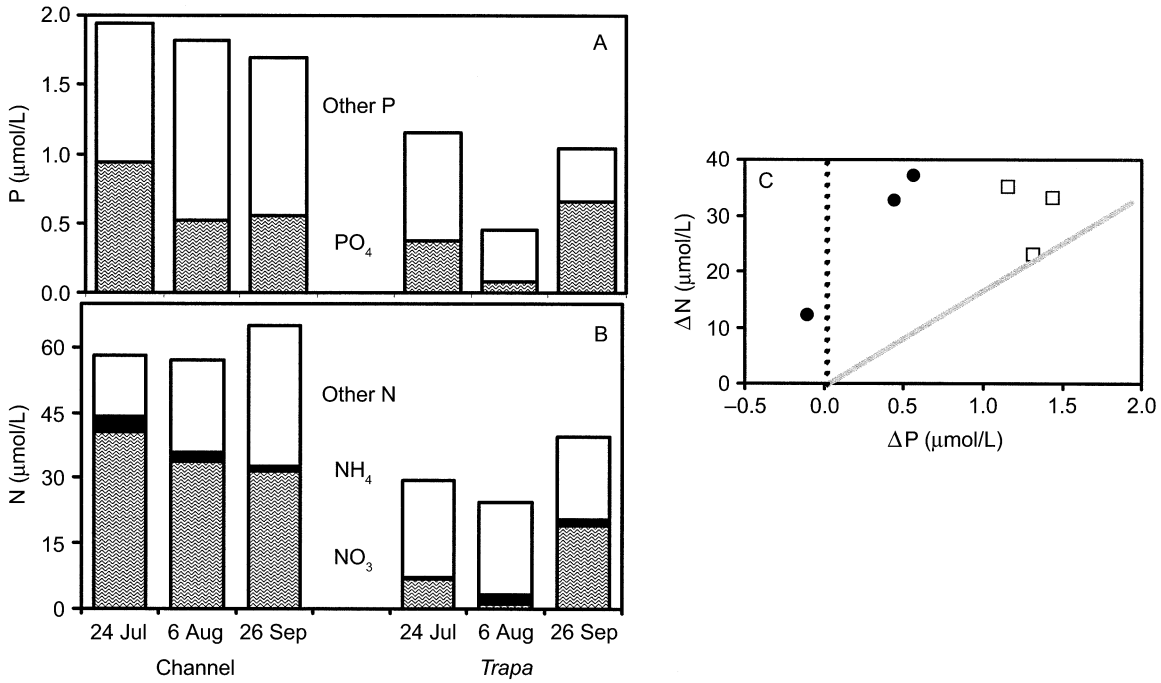


FIG. 8. Concentrations of (A) phosphorus and (B) nitrogen in the channel and a large *Trapa* bed (Fig. 1) during ebbing tide for three dates in summer 2000. The entire bar is total nutrient values, and ''other'' is the difference between measured nutrient species and total values. (C) The difference between channel and *Trapa* N concentrations (ΔN) vs. the P difference (ΔP). The dotted line represents no P difference, and the gray line is for N:P changing at a ratio of 16:1.

were 0.5 m, DO could increase to 5 mg/L by advective inputs alone during the flood tide. Dispersive inputs that occur would increase further the DO input during flooding tide and depend strongly on $F$ values (Eq. 4). These inputs are considered in the context of their impact on DO dynamics.

We were able to model the DO dynamics in the *Vallisneria* bed well in a scenario that considered only NEP and Adv. and considered Disp. and Atm. to be zero (Fig. 9C; Table 2, *S*1). For these conditions the model predicted diurnal DO changes from 7.2 to 9.8 mg/L with low values near sunrise to highest values at the low tide just prior to sunset (Fig. 9C). Actual data show diurnal range of 7.0–9.7 mg/L for the same time period (Fig. 6B). The model also predicted the lack of a smooth rise in DO during the day, which in the model is driven by proportionally higher production at low than high tides and advective inputs of channel DO during flooding tides. Including Atm. at maximum likely values or Disp. with $F \leq 0.5$ did not substantially alter model output as *Vallisneria* DO were not greatly different from either channel DO or atmospheric saturation (8.5 mg/L). Higher $F$ values caused the daytime peak DO to narrow and decrease in magnitude. For example, at $F = 3$ the modeled peak daytime DO is only 8.4 mg/L.

TABLE 2. Model output of net ecosystem production (NEP) and average mean, minimum, and maximum DO for seven scenario runs that vary plant or plant tissue (Plant), light, atmospheric exchange (Atm.), and dispersion (Disp.).

| Scenario | Plant | Disp. ($F$) | Atm. ($k$) | Light ($T$) | NEP | DO | | |
|---|---|---|---|---|---|---|---|---|
| | | | | | | Mean | Min. | Max. |
| *S*1 | *Vallisneria* | 0.0 | 0.0 | 0.45 | 0.2 | 7.9 | 6.9 | 9.4 |
| *S*2 | *Trapa* (s.t.) | 0.0 | 0.0 | 0.01 | −7.2 | 3.2 | 0.0 | 4.9 |
| *S*3 | *Trapa* (s.t.) | 0.3 | 0.0 | 0.01 | −7.2 | 5.0 | 3.3 | 5.9 |
| *S*4 | *Trapa* (s.t.) | 3.0 | 0.0 | 0.01 | −7.2 | 6.8 | 6.2 | 7.3 |
| *S*5 | *Trapa* (s.t.) | 0.0 | 0.8 | 0.01 | −7.2 | 5.0 | 3.9 | 5.6 |
| *S*6 | *Trapa* (s.t.) | 0.0 | 0.0 | 0.10 | −1.1 | 6.0 | 3.6 | 8.0 |
| *S*7 | *Trapa* (w.p.) | 0.0 | 0.0 | 0.01 | −0.3 | 7.5 | 1.0 | 13.8 |

*Notes:* These inputs were varied by changing $F$, $k$, and $T$ in Equations 4–6, respectively. *Trapa* (s.t.) and (w.p.) refer to submersed tissue or whole plant, respectively. NEP is in g $O_2 \cdot m^{-2} \cdot d^{-1}$, and DO is in mg/L. Model output is average for a 14-d model run in July. Model DO output is shown for two days of the model run in Fig. 9C–F.

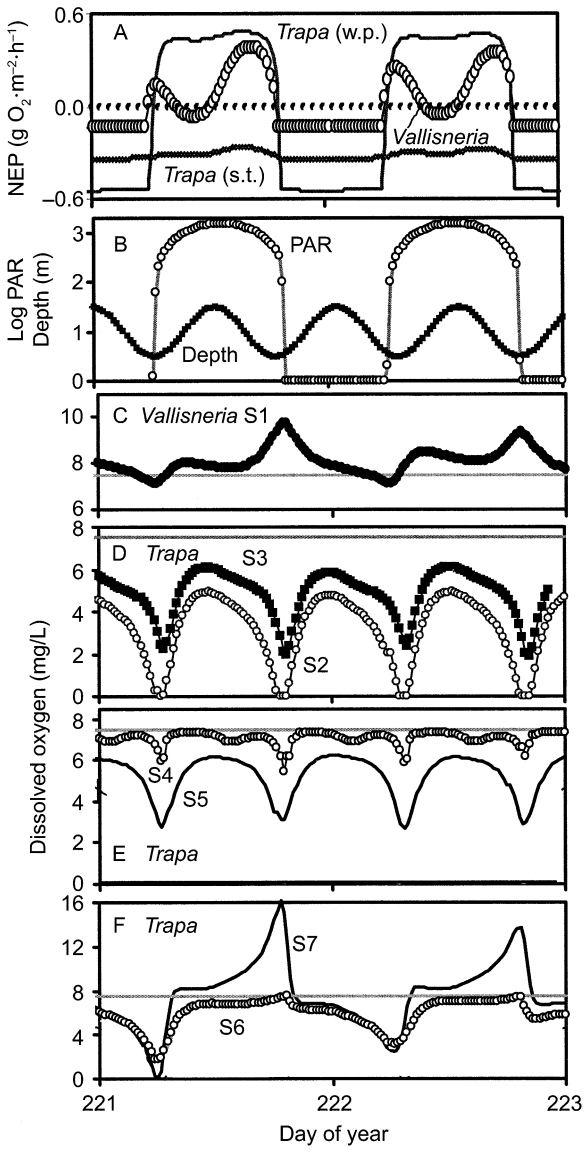


FIG. 9. Output of model for two days in July 2000. (A) Hourly net ecosystem production (NEP) for *Vallisneria* beds (open circles), *Trapa* beds including floating leaves (labeled *Trapa* (w.p.) [whole plant]), and for submersed *Trapa* tissue only (labeled *Trapa* (s.t.)). (B) Modeled incoming photosynthetically active radiation (PAR, open circles) and tidal variation in water column depth. Panels C–F show modeled DO for different model scenarios (*S*1–*S*7) described in Table 2. (C) Modeled DO variation in *Vallisneria* beds compared to a mean value of 7.5 mg/L in the channel (gray line). (D–F) Modeled DO variation in the *Trapa* bed for six different scenario runs (Table 2). Note that *S*1, *S*2, and *S*3 correspond well to actual measured DO dynamics in *Vallisneria* and at the inner and edge sites and the *Trapa* bed, respectively (Fig. 6).

DO dynamics at the inner site in the *Trapa* bed were modeled well considering only submersed tissue NEP and Adv. (Figs. 6C and 9D, *S*2). The model predicted dynamics to be tidally dominated with little diurnal pattern in DO dynamics. Low values of DO (0 mg/L) occur during each low tide and highs of near 5 mg/L during mid flood (Table 2, *S*2). For the edge site the higher DO values at low tide were predicted relatively well by adding a dispersive DO input driven by an $F = 0.3$; however, we predicted lower DO at high tide than were actually observed (Fig. 6C, Fig. 9D, *S*3; Table 2, *S*3). When substantially higher $F$ values were used we were able to model high DO at high tide, however, DO did not drop to the low values we observed at low tide (Fig. 9E, *S*4) and the tidal variation in DO when a value of $F = 3$ was used was only 1.5 mg/L. Inclusion of atmospheric exchange in the model also reduced tidal DO variation to less than that actually observed (Fig. 9E, *S*5)

In all model scenarios for *Trapa* where floating leaves were included in the DO balance of the water column, resulting DO dynamics did not resemble observed dynamics in *Trapa* beds (Fig. 9F, *S*7). For these scenarios a strong diurnal pattern in DO is predicted with DO dropping to <4 mg/L and rising to up to 16 mg/L. Inclusion of Atm. and Disp. dampens this diurnal pattern but still predicts a diurnal rather than a tidally based pattern in DO, and predicts far higher average DO values than we have observed in *Trapa* beds. A diurnal pattern of DO dynamics with higher than observed average DO is also modeled if we increase light penetration in beds as might occur in less dense beds of *Trapa*. For example, if we run a model scenario with 90% of light being absorbed in the surface layer rather than the 99% we measure ($T = 0.1$ vs. $= 0.01$, Eq. 6), we predict a diurnal pattern in DO with DO remaining near 7.5 mg/L throughout daylight hours and declining to 2–4 mg/L during nighttime low tides (Fig. 9F, *S*6).

## DISCUSSION

Our data clearly demonstrate strong differences in DO dynamics between macrophyte beds dominated by different species (Figs. 5 and 6). These differences include the pattern of DO cycling and, most importantly, the frequency of low DO events that can be harmful to fish and invertebrates. Low DO events were common in the beds dominated by the introduced species (*Trapa natans*) but never occurred in beds of the native (*Vallisneria americana*). Our model could reproduce the very different DO dynamics of *Vallisneria* beds and *Trapa* beds (Table 2, *S*1 vs. *S*2) with all aspects of the model identical except the balance between GPP and $R$ of submersed plant tissue (daytime NPP); sediment and watercolumn GPP and $R$ and Adv., Disp. and Atm. were identical between scenario runs 1 and 2 (Fig. 9C, D). Further, the different plant $R$ and GPPs in these scenario runs are based on measurements made in this study (Table 1, Figs. 3, 4) and were not manipulated parameters within the model. The low NPP of submersed *Trapa* tissue (GPP $-$ $R$) is due to high biomass of floating leaves that allow only 1% of incoming solar radiation to reach submersed leaves (Fig. 4).

According to our model, the strong DO decline in

*Trapa* beds during daytime ebbing tides is dependent on the high degree of shading by emergent leaves. Using our model to investigate this impact, we found that for *Trapa* beds that were not so dense and allowed even 10% of incoming light to penetrate through the water column, NEP during daytime would be balanced rather than negative and the occurrence of low DO events would be less frequent and less severe (Fig. 9F). Many of the smaller *Trapa* beds in the Hudson appear to have a higher percentage of open water (and are less dense). This difference in plant density, in addition to higher dispersive water exchange in smaller beds, could explain why we did not observe extremely low DO in small *Trapa* beds (Fig. 7). Whatever the cause, low DO events may be limited to the ~3 $km^2$ of the river occupied by large *Trapa* beds rather than the full 6 $km^2$ occupied by beds of all sizes. The 3-$km^2$ area represents ~15% of the total macrophyte area in the tidal freshwater Hudson. Hypoxia in these areas could have significant consequences.

In the Hudson, as is true in many systems, macrophyte beds are critical nursery habitats for fish (Kiviat 1993, Limburg et al. 1986). Both resident and anadromous fish rely heavily on these beds for the development of the juveniles, which are abundant during July to September. Hypoxia in macrophyte beds during this time-period is potentially of substantial significance. A preliminary study suggested that many juvenile fish, including striped bass (*Morone saxatillas*), and many clupeid species, forage in *Trapa* beds during high tide but are leaving beds during ebbing tide (T. W. Coote 2000, *unpublished manuscript* [report to the Polgar Fellowship Foundation: Use of a periodically anoxic *Trapa* bed by fishes in the Hudson River]). These species may face substantial predation risk as they leave the cover of beds. This danger could be accentuated, as the water leaving *Trapa* beds at the end of ebb tide has turbidities of only 1–3 NTU (~10× lower than the main channel of the river, Fig. 7A). The relatively clear water at the edge of the *Trapa* bed could enhance the risk of predation by visual predators, including birds and larger fish.

In addition to impacting the quality of macrophyte beds as habitats, low DO can also impact biogeochemical cycles within *Trapa* beds. For example, the alternation between oxic and hypoxic conditions may enhance denitrification, which can increase gaseous losses of N (Knowles 1982, Seitzinger and Kroeze 1998). In agreement with this possibility, preliminary measurements of nitrate levels within *Trapa* beds were <30% of nitrate levels in the main channel of the Hudson during July to September while $PO_4$ depletions were proportionally far lower (Fig. 8). The low $NO_3$ in *Trapa* beds suggests that these beds may be important sinks for N. In the ~3 $km^2$ of large *Trapa* beds within the tidal Hudson, at least $0.6 \times 10^7$ $m^3$ of water enter and leave the *Trapa* beds each day due to daily tidal movement. Thus, given an N depletion of 30 μmol/L in *Trapa* beds, about $1.8 \times 10^8$ mmol of $NO_3$ per day may be consumed in beds. This represents ~20% of the average daily summertime export of N from the tidal freshwater Hudson (Lampman et al. 1999) or close to all of the N entering this section of the river in point sources (Lampman et al.1999). If this N is being consumed by plant uptake it can potentially be made available after plant decline in the fall. If the N is being consumed by denitrification, it not only implies that *Trapa* beds could be hot spots of nitrous oxide production in the river (Cole and Caraco 2001) but also that the N depletion could be a more permanent sink. Thus, the hypoxia caused by *Trapa* could have significant geochemical as well as habitat consequences to the Hudson.

Hypoxia can occur in the absence of human activity, but it is well recognized that human activity can increase the frequency, extent, or duration of hypoxic events (D'Elia 1987). In general, two human activities are frequently associated with increased hypoxia in aquatic systems. First, the direct load of organics or other reduced substance to aquatic systems can consume DO throughout the water column (Clark et al. 1995). Second, humans can load nutrients to nutrient limited aquatic system and the greater production, and subsequent export, of organic material to bottom waters frequently leads to hypoxia (Elmgren 1989, Rabalais et al. 1996). Other human induced causes of hypoxia, including species introductions, are not widely recognized, and indeed the importance of individual species to the control of ecosystem function has only recently become widely recognized (e.g., Jones et al. 1997, Vanni et al. 1997, Vitousek et al. 1997, Strayer et al. 1999, Vander Zanden et al. 1999). To date, there are only a few studies that have linked species introductions with DO declines (Effler et al. 1998, Caraco et al. 2000), and we know of no other studies that have linked these introductions to severe hypoxia. This study demonstrates this connection for a large aquatic system.

## Acknowledgments

This is a contribution to the Institute of Ecosystem Studies. This research was supported by grants from the Hudson River Foundation, New York Sea Grant, the National Science Foundation, and the A. W. Mellon Foundation. The work benefited from discussions with S. Findlay, R. Garritt, C. Neider, E. Kiviat, and D. Strayer. We thank G. Lampman, A. Nixon, and D. Fischer for field and laboratory assistance. The manuscript was greatly improved by editorial comments of W. M. Kemp and comments of two anonymous reviewers. This work is a contribution to the Institute of Ecosystem Studies.

## Literature Cited

Caraco, N. F., J. J. Cole, S. E. G. Findlay, D. T. Fischer, G. G. Lampman, M. L. Pace, and D. L. Strayer. 2000. Dissolved oxygen declines in the Hudson River associated with the invasion of the zebra mussel (*Dreissena polymorpha*). Environmental Science and Technology **34**:1204–1210.

Caraco, N. F., J. J. Cole, P. A. Raymond, D. L. Strayer, M. L. Pace, S. E. G. Findlay, and D. T. Fischer. 1997. Zebra

mussel invasion in a large, turbid river: phytoplankton response to increased grazing. Ecology **78**:588–602.
Carpenter, S. R. 1980. Enrichment of Lake Wingra, Wisconsin, by submersed macrophyte decay. Ecology **61**:1145–1155.
Cataneo, A., G. Galanti, S. Gentinetta, and S. Romo. 1998. Epiphytic algae and macroinvertebrates on submerged and floating-leaved macrophytes in an Italian lake. Freshwater Biology **39**:725–740.
Clark, J. F., H. J. Simpson, R. F. Bopp, and B. L. Deck. 1995. Dissolved oxygen in lower Hudson estuary: 1978–93. Journal of Environmental Engineering **121**:760–763.
Cole, J. J., and N. F. Caraco. 2001. Emissions of nitrous oxide ($N_2O$) from a tidal, freshwater river; the Hudson River, New York. Environmental Science and Technology **35**:991–996.
Cole, J. J., N. F. Caraco, and B. L. Peierls. 1992. Can phytoplankton maintain a positive carbon balance in a turbid, freshwater, tidal estuary? Limnology and Oceanography **37**:1608–1617.
Cole, J. J., M. L. Pace, S. R. Carpenter, and J. F. Kitchell. 2000. Persistence of net heterotrophy in lakes during nutrient addition and food web manipulations. Limnology and Oceanography **45**:1718–1730.
D'Elia, C. F. 1987. Too much of a good thing: nutrient enrichment of the Chesapeake Bay environment. Environment **29**:6–11 + 30–33.
Duarte, C. M., and J. Cebrian. 1996. The fate of marine autotrophic production. Limnology and Oceanography **41**: 1758–1766.
Effler, S. W., S. R. Boone, C. Siegfried, and S. L. Ashby. 1998. Dynamics of zebra mussel oxygen demand in Seneca River, New York. Environmental Science and Technology **32**:807–812.
Elmgren, R. 1989. Baltic Sea changes—man's impact on the ecosystem of the sea: energy flow today and at the turn of the century. Ambio **18**:326–332.
France, R. L. 1995. Differentiation between littoral and pelagic food webs in lakes using stable carbon isotopes. Limnology and Oceanography **40**:1310–1313.
Frodge, J. D., G. L. Thamas, and G. B. Pauley. 1990. Effects of canopy formation by floating and submergent aquatic macrophytes on the water quality of two shallow Pacific Northwest lakes. Aquatic Botany **38**:231–248.
Garritt, R. H. 1990. The metabolism of a submersed macrophyte community in the tidal freshwater Hudson River estuary. Thesis. Cornell University, Ithaca, New York, USA.
Goldsborough, W. J., and W. M. Kemp. 1988. Light responses of a submersed macrophyte: implications for survival in turbid tidal waters. Ecology **69**:1775–1786.
Graneli, W., and D. Solander. 1988. Influence of aquatic macrophytes on phosphorus cycling in lakes. Hydrobiologia **170**:245–266.
Harley, M. T., and S. Findlay. 1994. Photosynthetic-irradiance relationships for three species of submersed macrophytes in the tidal freshwater Hudson River. Estuaries **17**: 200–205.
Iqbal, M. 1983. An introduction to solar radiation. Academic Press, San Diego, California, USA.
Jones, C. G., J. H. Lawton, and M. Shachak. 1997. Positive and negative effects of organisms as physical ecosystem engineers. Ecology **78**:1946–1957.
Kaenel, B. R., H. Buehrer, and U. Uehlinger. 2000. Effects of aquatic plant management on stream metabolism and oxygen balance in streams. Freshwater Biology **45**:85–95.
Kelly, V. 1993. Environmental monitoring program 1988–92 summary report. Part I. Meteorology and ozone. Occasional Publication of the Institute of Ecosystem Studies **8**:1–16.
Kemp, W. M., W. R. Boynton, R. R. Twilley, J. C. Stevenson, and L. G. Ward. 1984. Influence of submersed vascular plants on ecological processes in upper Chesapeake Bay. Pages 367–394 *in* V. S. Kennedy, editor. Estuaries as filters. Academic Press, San Diego, California, USA.
Kemp, W. M., P. Sampou, J. Caffey, M. Mayer, K. Henriksen, and W. R. Boynton. 1990. Ammonium recycling versus denitrification in Chesapeake Bay sediments. Limnology and Oceanography **35**:1545–1563.
Kiviat, E. 1993. Under the spreading water-chestnut. Hudsonia **9**:1–7.
Knowles, R. 1982. Denitrification. Microbiological Review **46**:43–70.
Lampman, G., N. Caraco, and J. Cole. 1999. Spatial and temporal patterns of nutrient concentration and export in the tidal Hudson River. Estuaries **22**:285–296.
Limburg, K. E., M. A. Moran, and W. H. McDowell. 1986. The Hudson River ecosystem. Springer-Verlag, New York, New York, USA.
Lovley, D. R. 1993. Anaerobes into heavy metal: dissimilatory metal reduction in anoxic environments. Trends in Ecology and Evolution **8**:193–227.
Miranda, L. E., M. P. Driscoll, and M. S. Allen. 2000. Transient physicochemical microhabitats facilitate fish survival in inhospitable aquatic plant stands. Freshwater Biology **44**:617–628.
Miranda, L. E., and K. B. Hodges. 2000. Role of aquatic vegetation coverage on hypoxia and sunfish abundance in bays of a eutrophic reservoir. Hydrobiologia **427**:51–57.
Moore, B. C., W. H. Funk, and E. Anderson. 1994. Water quality, fishery, and biologic characteristics in a shallow, eutrophic lake with dense macrophyte populations. Lake and Reservoir Management **8**:175–188.
Muenscher, W. C. 1935. Aquatic vegetation of the Mohawk–Hudson watershed. Pages 228–242 *in* State of New York Conservation Department, editor. A biological survey of the Mohawk–Hudson watershed. Biological Survey IX. J. B. Lyon, Albany, New York, USA.
Muenscher, W. C. 1937. Aquatic vegetation of the lower Hudson area. Pages 231–238 *in* State of New York Conservation Department, editor. A biological survey of the lower Hudson watershed. Biological Survey XI. J. B. Lyon, Albany, New York, USA.
Pokorny, J., and E. Rejmankova. 1984. Oxygen regime in a fish pond with duckweeds Lemnaceae and Ceratophyllum. Aquatic Botany **17**:125–138.
Rabalais, N. N., R. E. Turner, D. Justic, Q. Dortch, W. J. Wiseman, Jr., and B. K. Sen Gupta. 1996. Nutrient changes in the Mississippi River and system responses on the adjacent continental shelf. Estuaries **19**:386–407.
Roland, F., N. F. Caraco, J. J. Cole, and P. del Giorgio. 1999. Rapid and precise determination of dissolved oxygen by spectrophotometry: evaluation of interference from color and turbidity. Limnology and Oceanography **44**:1148–1154.
Seitzinger, S. P., and C. Kroeze. 1998. Global distribution of nitrous oxide production and N inputs in freshwater and coastal marine ecosystems. Global Biogeochemical Cycles **12**:93–113.
Sondergaard, M., and K. Sand-Jensen. 1979. Total autotrophic production in oligotrophic Lake Kalgaard, Denmark. Verhandlungen Internationale Vereinigung für Theoretische und Angewandte Limnologie **20**:667–673.
Strayer, D. L., N. F. Caraco, J. J. Cole, S. Findlay, and M. L. Pace. 1999. Transformations of freshwater ecosystems by bivalves: a case study of zebra mussels in the Hudson River. BioScience **49**:19–28.
Suthers, I. M., and J. H. Gee. 1986. Role of hypoxia in limiting diel spring and summer distribution of juvenile yellow perch Perca-flavensecens in a prairie marsh. Canadian Journal of Fisheries and Aquatic Sciences **43**:1562–1570.

Valiela, I., K. Foreman, M. LaMontagne, D. Hersh, J. Costa, P. Peckol, B. DeMeo-Anderson, C. D'Avanzo, M. Babione, C.-H. Sham, J. Brawley, and K. Lajtha. 1992. Couplings of watersheds and coastal waters: sources and consequences of nutrient enrichment in Waquoit Bay, Massachusetts. Estuaries **15**:443–457.

Vander Zanden, M. J., J. M. Casselman, and J. B. Rasmussen. 1999. Stable isotope evidence for the food web consequences of species invasion in lakes. Nature **401**:464–466.

Vanni, M. J., C. D. Layne, and S. E. Arnott. 1990. ''Top-down'' trophic interactions in lakes: effects of fish on nutrient dynamics **78**:1–20.

Vitousek, P. M., C. M. D'Antonia, L. L. Loope, and R. Westbrooks. 1997. Biological invasions as global environmental change. American Scientist **84**:468–478.

Welcomme, R. L. 1995. River fisheries. FAO fisheries, Technical Report 262.

Wetzel, R. G. 1983. Limnology. Second edition. Saunders, Philadelphia, Pennsylvania, USA.

Wilcock, R. J., P. D. Champion, J. W. Nagels, and G. F. Croker. 1999. The influence of aquatic macrophytes on the hydraulic and physico-chemical properties of a New Zealand lowland stream. Hydrobiologia **416**:203–214.